Long-term exposure of A549 cells to titanium dioxide nanoparticles induces DNA damage and sensitizes cells towards genotoxic agents

Armand, Lucie; Tarantini, Adeline; Beal, David; Biola-Clier, Mathilde; Bobyk, Laure; Sorieul, Sephanie; Pernet-Gallay, Karin; Desvergne, Caroline; Lynch, Iseult; Herlin-Boime, Nathalie; Carriere, Marie

DOI:
10.3109/17435390.2016.1141338

License:
Other (please specify with Rights Statement)

Document Version
Peer reviewed version

Citation for published version (Harvard):
Armand, L, Tarantini, A, Beal, D, Biola-Clier, M, Bobyk, L, Sorieul, S, Pernet-Gallay, K, Desvergne, C, Lynch, I, Herlin-Boime, N & Carriere, M 2016, 'Long-term exposure of A549 cells to titanium dioxide nanoparticles induces DNA damage and sensitizes cells towards genotoxic agents', *Nanotoxicology*.
https://doi.org/10.3109/17435390.2016.1141338

Long-term exposure of A549 cells to titanium dioxide nanoparticles induces DNA damage and sensitizes cells towards genotoxic agents

Lucie Armand[1,2], Adeline Tarantini[1,2], David Beal[1,2], Mathilde Biola-Clier[1,2], Laure Bobyk[1,2], Sephanie Sorieul[3], Karin Pernet-Gallay[4,5], Caroline Marie-Desvergne[6], Iseult Lynch[7], Nathalie Herlin-Boime[8], Marie Carriere[1,2,§]

[1]Université Grenoble-Alpes, INAC-LCIB, Laboratoire Lésions des Acides Nucléiques, 17 rue des Martyrs, F-38000 Grenoble, France.

[2]CEA, INAC-SCIB, Laboratoire Lésions des Acides Nucléiques, 17 rue des Martyrs, F-38000 Grenoble, France.

[3]CENBG, Université Bordeaux 1, IN2P3, UMR5797, 33175 Gradignan Cedex, France.

[4]Université Grenoble Alpes, Grenoble Institut des Neurosciences, Grenoble F-38000, France

[5]INSERM U 836, F-38000 Grenoble, France.

[6]Université Grenoble-Alpes, CEA, Nanosafety Platform, Medical Biology Laboratory (LBM), 17 rue des Martyrs, F-38054 Grenoble, France.

[7]School of Geography, Earth and Environmental Sciences, University of Birmingham, Edgbaston, B15 2TT Birmingham, United Kingdom

[8]UMR3685 CEA-CNRS, NIMBE, LEDNA, CEA Saclay, F-91191 Gif sur Yvette, France.

[§]Corresponding author: Marie Carrière, CEA Grenoble, LAN, Bât C5, pce 632, 38054 Grenoble Cedex 9, France. Phone: +33 4 38 78 03 28, fax: +33 4 38 78 50 90. marie.carriere@cea.fr

Keywords

Nanoparticle, TiO_2, toxicity, genotoxicity, chronic

Abstract

Titanium dioxide nanoparticles (TiO_2-NPs) are one of the most produced NPs in the world. Their toxicity has been studied for a decade using acute exposure scenarios, i.e. high exposure concentrations and short exposure times. In the present study, we evaluated their genotoxic impact using long-term and low concentration exposure conditions.

A549 alveolar epithelial cells were continuously exposed to 1-50 µg/mL TiO_2-NPs, 86% anatase / 14% rutile, 24±6 nm average primary diameter, for up to two months. Their cytotoxicity, oxidative potential and intracellular accumulation were evaluated using MTT assay and reactive oxygen species measurement, transmission electron microscopy observation, micro-particle-induced X-ray emission and inductively-coupled plasma mass spectroscopy. Genotoxic impact was assessed using alkaline and Fpg-modified comet assay, immunostaining of 53BP1 foci and the cytokinesis-blocked micronucleus assay. Finally, we evaluated the impact of a subsequent exposure of these cells to the alkylating agent methyl methanesulfonate.

We demonstrate that long-term exposure to TiO_2-NPs does not affect cell viability but causes DNA damage, particularly oxidative damage to DNA and increased 53BP1 foci counts, correlated with increased intracellular accumulation of NPs. In addition, exposure over 2 months causes cellular responses suggestive of adaptation, characterized by decreased proliferation rate and stabilization of TiO_2-NP intracellular accumulation, as well as sensitization to MMS. Taken together, these data underline the genotoxic impact and sensitization effect of long-term exposure of lung alveolar epithelial cells to low levels of TiO_2-NPs.

Introduction

Titanium dioxide nanoparticles (TiO_2-NPs) are present in everyday products such as sunscreens, sweets and paints (Shi, 2013). Since their production volume is predicted to exceed that of TiO_2 microparticles (Robichaud, 2009), increased occupational and environmental exposure of the population to these NPs is expected. To date, NP toxicology studies have mainly focused on the lung, as inhalation is the most likely and most concerning NP exposure mode. NPs and ultrafine particles show similar physico-chemical properties, which suggests that NPs may be carcinogenic just like ultrafine particles (Loomis, 2013). Epidemiological studies so far failed to demonstrate a direct link between exposure to TiO_2-NPs and cancer development (Baan, 2007). This is why IARC, in its monograph on the evaluation of carcinogenic risks to human from carbon black, titanium dioxide and talc, concluded that "there is inadequate evidence in humans for the carcinogenicity of titanium dioxide", while they concluded on "sufficient evidence in experimental animals for the carcinogenicity of titanium dioxide", which supported the overall evaluation that "titanium dioxide is possibly carcinogenic to humans (Group 2B)" (IARC, 2010). Still many *in vitro* and *in vivo* studies focus on TiO_2-NP genotoxicity as a hallmark of early carcinogenicity. The conclusions of these genotoxicity or DNA damage studies are conflictive (IARC, 2010; Shi, 2013) probably because NPs with various physicochemical characteristics are used. Additionally, even if the same NP is used, the dispersion procedure, depending on the composition of the dispersion medium and the time of sonication, may lead to significant differences in NP agglomerate sizes and coatings and consequently in NP biological effects. In particular, it is now well documented that addition of proteins such as BSA or serum leads to coating of the NPs with proteins which stabilize the NP suspension but also may mask reactive sites on NP surface, thus reducing their short-term cyto- or genotoxicity (Carriere, 2014; Magdolenova, 2012). However, the situation may differ upon long-term exposure, since long-term NP accumulation in lysosomes may cause corona proteins degradation and consequently NP surface may get revealed again. In addition to these conflicting results, *in vitro* exposure scenarios are most of the time unrealistic, i.e. exposure concentrations range between 5 µg/mL and 100 µg/mL and exposure times are very short, i.e. less than 24 h (Chen, 2014). This exposure concentration is 10^6-fold higher than human inhalation exposure even in a worst-case scenario (Paur, 2011), and individuals are exposed to TiO_2-NPs during

their whole life (Weir, 2012). This therefore raises the question of the accuracy of acute exposure models, since biological effects and related mechanisms may differ depending on exposure concentration and time.

Interesting results recently emerged from long-term, chronic *in vitro* exposure scenarios, representing an important breakthrough in nanotoxicology literature. Exposure of a human keratinocyte cell line to 5 µg/mL of 25 nm anatase TiO_2-NPs for up to 3 months caused neither overt cytotoxicity nor reactive oxygen species accumulation (Kocbek, 2010). A 3-week exposure of human mesenchymal stem cells to TiO_2-NPs also did not induce significant cytotoxic impact (Hackenberg, 2013). However it induced the formation of nanotubular protrusions of the exposed cells' plasma membranes and increased the proportion of cells in the subG1 phase of the cell cycle (Kocbek, 2010). Modification of cell cycle progression was also observed in Chinese Hamster Ovary cells (CHO-K1) continuously exposed to 10-40 µg/mL of anatase TiO_2-NPs for 2 months, with an increased proportion of cells in the G2/M phase. In this cell line, chronic exposure to TiO_2-NPs impacted neither cell proliferation and survival nor caused genotoxic events, but correlated with reactive oxygen species accumulation in exposed cells (Wang, 2011). Exposure of NIH3T3 fibroblasts to 10 µg/mL TiO_2-NPs for up to 3 months impaired cell cycle progression and mitosis, and altered genome segregation due to interference of NPs with mitotic spindle assembly and with centrosome maturation. The authors concluded that long-term exposure to TiO_2-NPs thus induced cell transformation and chromosomal instability, via deregulation of PLK1 function (Huang, 2009). Finally, exposure of BEAS-2B bronchial cell line for 4 weeks to anatase TiO_2-NPs (NM102 representative material from the Joint Research Center, Ispra, Italy) induced neither primary lesions and oxidative damage to DNA, nor chromosomal damage. However, they induced cell transformation in the soft-agar plate assay (Vales, 2014).

In this context, the present study was designed to assess possible genotoxicity of TiO_2-NPs upon long-term, 8-week continuous exposure of A549 lung alveolar cells. The rationale for using this cell line is that 20 nm-diameter NPs are expected to reach the alveolar compartment of the lung rather than the bronchial compartment (Shi, 2013). Moreover we used TiO_2-NPs with mix anatase/rutile crystalline phases (NM105 from the Joint Research Center, Ispra, Italy, i.e. P25 Aeroxide from Evonik), which are more reactive than pure anatase TiO_2-NPs (Gerloff, 2009) and show the highest stability of well-dispersed suspensions upon

dispersion via sonication (Jugan, 2012; Simon-Deckers, 2008). We previously demonstrated that these TiO_2-NPs caused cytotoxicity and genotoxicity in this cell line upon acute exposure, *in vitro* (Jugan, 2012; Simon-Deckers, 2008). Moreover they caused drastic reduction of cellular ability to repair damaged DNA (Jugan, 2012). Our previous work, using 2D-gel electrophoresis analysis together with functional validation to analyze the molecular response of A549 cells to 2 months, chronic exposure to these NPs, showed that this exposure scenario impacts the abundance of 22 gene products involved in glucose metabolism, trafficking, gene expression, mitochondrial function, proteasome activity and DNA damage response (Armand, 2015). This chronic exposure was also found to increase the intracellular content of the serine-threonine kinase receptor-associated protein (STRAP) whose role is to stabilize p53 coactivators p300 and JMY so that they activate p53, which are indicative of DNA damage. Moreover, p53 phosphorylation and acetylation were increased, leading to cell cycle slowdown (Armand, 2015).

In the present study, we investigated the impact of these TiO_2-NPs on DNA stability, also using a chronical 2-months exposure scenario. Our initial aim was to analyze the impact of very low TiO_2-NP concentrations, in the range of 1 ng/mL to 50 µg/mL. However, since our first results showed that the biological response to 2 months exposure to 1 µg/mL TiO_2-NPs was insignificant, we decided to focus subsequent studies on the range inducing a dose-dependent cellular response, i.e. 1-50 µg/mL TiO_2-NPs. We characterized TiO_2-NP cellular accumulation and distribution using transmission electronic microscopy (TEM), micro particle-induced X-ray emission (µPIXE) and ICP-MS. Cell viability and redox status were assessed after exposure. Moreover, we characterized the genome instability caused by this exposure model, by using (1) the comet assay in its alkaline and Fpg-modified versions to probe DNA strand breaks, alkali-labile sites and Fpg-sensitive sites including 8-oxo-dGuo, (2) 53BP1 foci numeration to probe DNA double-strand breaks and DNA replication fork blockade, and (3) the cytokinesis-blocked micronucleus assay to probe clastogenic and aneugenic events. Finally, we assessed sensitization towards the alkylating agent methane-methyl sulfonate (MMS) that this long-term exposure to TiO_2-NPs provides, by first exposing cells for 2 months to TiO_2-NPs then exposing them to a sublethal concentration of MMS, and characterizing cell viability and DNA integrity.

Together these identify a large range of potential NP-induced DNA damage mechanisms and allow a very detailed picture of key steps to be elucidated.

Methods

Nanoparticle dispersion and characterization

TiO_2-NPs (AEROXIDE® P25, Evonik) were obtained from the library of the Joint Research Center (JRC, Ispra, Italy) where they are designated NM105. They were dispersed in ultrapure sterile water to the concentration of 10 mg/mL, by high power probe sonication in pulsed mode (1s on/1s off), at 4°C and 28% of amplitude, over 30 min as described previously (Carriere, 2014; Simon-Deckers, 2008). The power delivered by our sonicator at 28% of amplitude is 16.8 W (Brun, 2014). Suspensions were stored in the dark at room temperature. Just before cell exposure, the suspension was vigorously vortexed and diluted in exposure medium, i.e. DMEM containing 10% fetal bovine serum (FBS). The hydrodynamic diameter of the TiO_2-NPs diluted to 5 µg/mL in ultrapure water or exposure medium was determined by dynamic light scattering (DLS) on a ZetaSizer Nano ZS (Malvern, Worcestershire, UK). Size and size distribution was analyzed immediately following dispersion and over the timecourse of the exposure (after 2 months).

Cell culture

A549 human lung carcinoma cells were purchased from ATCC (Manassas, VA, USA, reference CCL-185) and grown in DMEM 4.5 g/L glucose (Life Technologies, Carlsbad, CA, USA) containing 2 mM/L glutamine, penicillin/streptomycin (50 IU/mL and 50 mg/ml respectively) and 10% FBS. They were maintained at 37°C in a 5% CO_2/air incubator.

NP exposure

Over a period of up to 2 months, cells were subcultured in cell culture medium containing freshly-diluted NPs twice a week (Figure S1), using the following protocol: wells were rinsed with PBS, trypsinized with trypsin-EDTA 0.25% and counted after trypan blue staining. Cells were then seeded in a new dish (seeding details described in the specific experimental protocols below), in cell culture medium containing

1, 2.5, 5, 10 or 50 µg/mL TiO_2-NPs, these concentrations being in line with those used in the previously published TiO_2-NP chronic exposure studies (Huang, 2009; Kocbek, 2010; Vales, 2014; Wang, 2011). The 10 mg/mL NP stock suspension (prepared in water) was the same during the whole exposure time. The dispersion state of the suspension was checked by DLS immediately after dispersion, then after 2 weeks, 1 month and 2 months; size distribution did not significantly evolve. Moreover TiO_2-NPs did not significantly dissolve over time, as attested by ICP-MS measurement of Ti ion content in the supernatant of the suspension (after ultracentrifugation at 400 000 *g* for 30 min; material and methods for ICP-MS are described in Electronic Supplementary Information) collected just after sonication and at the end of the 2 month experiments (not shown). After 24 hours, 1 week, 2 weeks, 1 month and 2 months of treatment, cells were seeded i) in well plates or microscope coverslips to carry out the cytotoxicity, genotoxicity, RT-qPCR and redox balance analyses experiments and ii) in petri dishes to continue the exposure experiment. Cells prepared for cytotoxicity, genotoxicity, RT-qPCR and redox balance analyses experiments were processed either immediately (MTT, trypan blue, H2DCFDA) or conditioned, stored and processed after completion of the 2 month exposure (ICP-MS, propidium iodide staining, redox enzyme activity, comet assay, 53BP1 and micronucleus assay). Storage conditions are described below and in Table S1. The whole chronic exposure experiment was repeated 4 times, independently, and most of the experiments described below were thus repeated 4 times independently, except TEM imaging which was performed once, and PIXE and ICP-MS measurement of TiO_2-NP intracellular accumulation which were repeated twice (for detailed number of independent experiment for each assay, see Table S1).

Cytotoxicity and cell proliferation

Cytotoxicity was assessed using the 3-[4,5-dimethylthiazol-2-yl]-2,5-diphenyl tetrazolium bromide (MTT) assay (Sigma-Aldrich, St. Louis, MO, USA). Cells were seeded at sub-confluence in 96-well plates, in cell culture medium containing 1, 2.5, 5, 10 or 50 µg/mL TiO_2-NPs (6 wells per condition). After 16-hours, to allow cell adhesion, the medium in each well was replaced by 0.5 mg/mL MTT diluted DMEM. After 1 h of incubation at 37°C, formazan crystals were dissolved in 100 µL DMSO. To limit interference NPs were then allowed to sediment for 1 h, after which the plate was centrifuged at 450 × *g* for 5 min. 50 µL per well was transferred to a new 96-well plate. Absorbance was measured at 570 nm and cell viability was

determined as percentage of absorbance of negative control (unexposed cells). Trypan blue count (2 replicates per condition) was used to calculate the population doubling level (PDL) at each exposure concentration and at each cell passage, using the following formula: $PDL = t*log2/(logN_t - logN_0)$ (N_0 and N_t being cell counts immediately after seeding and t days after seeding, respectively).

We also used propidium iodide staining to assess cell viability. After exposure to 0, 1, 2.5, 5, 10, 50 µg/mL TiO_2-NP, cells were collected (10^6 cells per condition, 4 replicates) and rinsed with PBS containing 2 mM EDTA (PBS-EDTA). Cells were fixed in ice-cold 70% ethanol for 30 min then washed with PBS-EDTA. They were suspended in PBS-EDTA containing 25 µg/mL propidium iodide (Life Technologies) and 25 µg/mL RNAse A (Sigma-Aldrich). A minimum of 20 000 events per condition was measured by flow cytometry using a FacsCalibur analyzer (BD Biosciences, Franklin Lanes, NJ, USA) equipped with CXP software (Beckman Coulter Inc., Pasadena, CA, USA). Median fluorescence was calculated using Flowing Software 2.5.1 (http://www.flowingsoftware.com/). Fluorescence intensity median results were normalized to untreated control.

Intracellular accumulation and distribution

NP accumulation and intracellular distribution were measured by µ-particle-induced X-ray emission (µPIXE) and Elastic Backscattering (EBS). Cells were seeded onto polycarbonate membranes and allowed to adhere for 16 h. They were then rinsed twice with PBS and cryofixed by immersion in isopentane chilled to -160°C in liquid nitrogen (Carriere, 2005). Samples were freeze-dried for 24 h at -10°C, 0.37 mbar. Micro-PIXE and EBS spectra were recorded simultaneously on the microbeam line of the AIFIRA platform (CENBG, Bordeaux, France) (Barberet, 2009). The 3.5 MV Singletron accelerator (HVEE) was adjusted in order to deliver a focused beam (2.5 µm in diameter) of 3 MeV protons with a beam current of 1 nA. X-rays were detected with an 80 mm^2 Si(Li) detector (Gresham) orientated at 135° with respect to the incident beam axis, and equipped with a 12 µm thick beryllium window. A funny filter (Al, thickness 200 µm, size hole = 1 mm) was used in order to limit the dead-time below 10%. Backscattered protons were recorded at 135° with a silicon PIPS detector (Canberra, 25 mm^2, thickness 100 µm, resolution: 17 keV). Four elemental maps of 100×100 $µm^2$ were recorded on each sample, and drawn using the SupaVISIO software (http://biopixe.free.fr). For Ti intracellular content measurement, data

were fitted using SIMNRA (EBS) (Mayer, 2002) and Gupix (X-ray spectra) (Campbell, 2010) as described previously and normalized by analysis of standards, kindly provided by Dr. R. Ortega.

Intracellular distribution was observed by TEM. After exposure cells were rinsed twice with PBS, fixed with 2% glutaraldehyde and 1% osmium tetroxide. They were then gradually dehydrated with ethanol and embedded in Epon resin. Sections were cut by ultramicrotomy (80 nm) and observed on a JEOL 1200EX TEM operating at 80 kV (Grenoble Institut des Neurosciences, Grenoble, France).

Oxidative stress

Oxidative stress was first evaluated through measurement of intracellular reactive oxygen species (ROS) formation, using the fluorescent 2',7'-dichlorodihydrofluorescein diacetate acetyl ester (H_2DCFDA, Life Technologies) probe. At each time-point of the long-term exposure (24 h, 1 week, 2 weeks, 1 months and 2 months) cells exposed to TiO_2-NPs were harvested and seeded in a new 12-well plate, in exposure medium containing the same concentration of TiO_2-NPs as during chronic exposure (4 replicates per condition). After 16 h, they were washed twice with PBS, incubated for 30 min at 37°C with 80 µM H_2DCFDA then harvested by scraping in 200 µL of PBS. 100 µL of each cell suspension was transferred to a black 96-well plate, and fluorescence intensity was immediately measured with excitation at 480 nm, emission at 530 nm and a cutoff at 515 nm, on a Spectramax M2 spectrophotometer (MTX Lab Systems, Vienna, VA, USA). Relative fluorescence was normalized with respect to protein concentration, which was measured on 20 µL of the cell suspensions to which was added 200 µL of Bradford reagent. Protein concentration was then established using a calibration curve prepared from 0-500 µg/mL of BSA. Hydrogen peroxide (H_2O_2) was used as a positive control, with exposure for 30 min at 50 µM. In order to estimate interference of TiO_2-NPs with this assay, the same protocol was applied to cells seeded and treated in exactly the same conditions but not incubated with H_2DCFDA. Some fluorescence of TiO_2-NPs was observed, but it accounted for less than 10% of the total fluorescence signal in the H2DCF-DA + NP treated cells.

In cell samples exposed to NPs for 2 months, glutathione concentration, both total (GSH+GSSG) and reduced (GSH), as well as the activity of the 4 antioxidant enzymes glutathione reductase (GR), glutathione peroxidase (GPx), superoxide dismutase (SOD) and catalase (CAT) were monitored as

previously described (Barillet, 2010), with 3 replicates per condition. For detailed protocols, see the Electronic Supplementary Information.

DNA damage

NP-induced DNA strand breaks and alkali-labile sites were assessed through the alkaline version of the comet assay (Singh, 1988). Oxidatively damaged DNA was quantified by using the bacterial DNA repair enzyme formamidopyrimidine-DNA glycosylase (Fpg) in the comet assay (Gurr, 2005). This enzyme converts oxidized purines, including the major purine oxidation product 8-oxoguanine, into single-strand breaks (SSB, therefore detectable by the comet assay) through a base-excision process (Collins, 2009). At the end of the exposure time, cells (1 well per condition) were rinsed three times with PBS, trypsinized, then pelleted by centrifugation for 5 min at 250 *g*. Cell pellets were then resuspended in sucrose 85.5 g/L, DMSO 50 mL/L prepared in citrate buffer (11.8 g/L), pH 7.6, and immediately frozen at -80°C. At the end of the 2 months exposure period, samples were thawn and processed as described hereafter for the comet assay. Six microscope slides per condition were coated with 1% normal melting point agarose (NMA) and allowed to dry. 10000 cells per slide were mixed with 0.6% low melting point agarose (LMPA) and deposited over the NMA layer. The cell/LMPA mix was then allowed to solidify on ice for 10 min. Slides were immersed in cold lysis solution (2.5 M NaCl, 100 mM EDTA, 10 mM Tris, 10% DMSO, 1% Triton X-100) overnight at 4°C, before being rinsed in 0.4 M Tris pH 7.4. Then 3 slides were treated with 100 µL Fpg (5 U/slide, in enzyme buffer, Trevigen, Gaithersburg, MD, USA) and 3 slides were incubated with Fpg enzyme buffer for 45 min at 37 °C. DNA was then allowed to unwind for 30 min in alkaline electrophoresis solution (300 mM NaOH, 1 mM EDTA, pH > 13). Electrophoresis was performed in an electric field of 0.7 V/cm and 300 mA for 30 min. Slides were then neutralized in 0.4 M Tris pH 7.4 and were stained with 50 µL of 20 mg/ml ethidium bromide (Life Technologies). As a positive control for alkaline comet assay, we used 50 µM H_2O_2 directly deposited onto the agarose layer containing the cells, incubated for 5 min at room temperature. As a positive control for comet-Fpg we used A549 cells exposed for 20 min at 37 °C to 1 µM riboflavin, then exposed to 10 J/cm² of UVA. At least 50 comets per slide were analyzed under a fluorescence microscope (Carl Zeiss, Oberkochen, Germany) connected to a charge-

coupled device camera with a 350-390 nm excitation and 456 nm emission filter, at x20 magnification. Comets were measured and analyzed using Comet IV software (Perceptive Instruments, Suffolk, UK).

To evaluate DNA double strand breaks (DSB) or replication fork blockade, p53 binding protein 1 (53BP1) foci were revealed and counted in cell nuclei. 53BP1 is a non-enzymatic protein which is recruited shortly after primary DSB detection. This protein is homogeneously distributed in the nuclei of unperturbed cells then it is recruited within 1-2 min to DSB sites (Bekker-Jensen, 2010); like gamma-H2AX it can therefore serve as a marker for DSB. As a positive control, we exposed cells to 25 µM etoposide (Sigma-Aldrich) for 24 h. Cells were fixed for 20 min in 3% paraformaldehyde (Sigma-Aldrich), stained using anti-53BP1 antibody (Novus Biologicals, Littleton, CO, USA, 1/500 vol./vol.) and slides were mounted with Fluoroshield (Sigma-Aldrich) containing DAPI (1 slides per condition). 53BP1 foci were visualized on an Axio ImageA1 microscope coupled to an Axiocam MRm camera (Carl Zeiss). At least 15 images per condition were captured; on each image we determined both total number of 53BP1 foci and total number of nuclei. Apoptotic cells and dividing cells were rejected.

The micronucleus assay, probing aneuploidic and clastogenic events, was performed as described previously (Fenech, 2000). Cells exposed to TiO_2-NPs were seeded on glass coverslips (3 coverslips per condition, i.e. 3 independent replicates). As a positive control, we used A549 cells exposed for 24 h to 100 µM methyl methanesulfonate (MMS, Sigma-Aldrich) (3 replicates). They were then cultured for another 28 h in culture medium (without NPs) containing 4 µg/ml cytochalasin B (Sigma-Aldrich) to block cytokinesis. Cells were then immediately fixed for 20 min in 3% paraformaldehyde and stained with acridine orange (5 mg/mL, Life Technologies) for 15 min. Coverslips were mounted on microscope slides with Fluoroshield mounting medium containing DAPI. At least 20 images per coverslip were captured with an Axio ImageA1 microscope (Carl Zeiss). On each image, total nr. of cells, binucleated cells and micronuclei were counted.

Statistical analysis

For each assay, the number of biological replicates per experiment as well as the number of 2 months exposure experiment in which the assay was done is summarized in Table S1. Except for TEM, µPIXE and ICP-MS assays, data curation was carried out as follows: results from biological replicates of each independent experiment were averaged; results presented in figures are mean ± s.e.m. of these averages.

For ICP-MS assay, the assay was performed only once, with 4 independent replicates. Data presented in Table S2 are thus mean ± s.e.m. of these 4 independent replicates. For µPIXE, 4 measurements were performed on each of the 2 independent samples (prepared during 2 independent 2 month exposure experiments); data presented in Figure 1 are the mean ± s.e.m. of the 8 values that were obtained. Statistical significance was assessed by Kruskal-Wallis non-parametric one-way analyses of variance by ranks, using the Statistica 8.0 software (Statsoft, Chicago, IL, USA). When significance was demonstrated ($p < 0.05$), paired comparisons were run using Mann-Whitney tests.

Results

Characterization of TiO_2 nanoparticles

The TiO_2-NPs used in the present study, P25 Aeroxide, have already been characterized in terms of morphology, primary size, surface specific area and isoelectric point (Jugan, 2012; Simon-Deckers, 2008). Briefly they are round-shaped (Figure S2) with an average primary particle diameter of 24±6 nm (as measured by TEM) and average specific surface area of 46±1 m^2/g. Their crystalline phase is 86% anatase and 14% rutile. We dispersed these NPs in water, using high energy sonication as previously described (Carriere, 2014; Simon-Deckers, 2008). After this dispersion stage in water, their average hydrodynamic diameter, measured by DLS and expressed in number, was 44±25 nm (Figure S2). Their polydispersity index (PdI) was 0.146±0.009. This distribution did not evolve significantly during the 2 months of the experiment; distribution profiles were almost identical 24 h and 2 months after dispersion (not shown). Just before each cell passage, after vigorous vortexing this suspension was diluted in cell culture medium containing 10% FBS to reach NP concentrations of 1, 2.5, 5, 10 or 50 µg/mL. In this exposure medium their zeta potential was -11.2±0.8 mV; their hydrodynamic diameter increased to 342±15 nm and PdI increased to 0.236±0.048, indicating that NPs agglomerated somewhat (Figure S2).

NP accumulation and distribution in exposed cells

In order to characterize the interaction between TiO_2-NPs and cells, we evaluated their cellular accumulation and distribution. Micro-PIXE showed that every cell contained Ti whatever the exposure time (Figure 1A). Indeed Ti-rich areas co-localized with K/Ca-rich areas which represent the outlines of cells.

Integration of PIXE spectra (Figure 1B), recorded on 4 different samples per condition, showed that Ti accumulation was significant at both 2.5 and 50 µg/mL and that it was higher in cells exposed to 50 µg/mL TiO_2-NPs than in cells exposed to 2.5 µg/mL TiO_2-NPs (Figure 1C). Moreover in cells exposed to 50 µg/mL TiO_2-NPs, Ti content was higher after 1 month of exposure than after 24 h of exposure. Then it did not increase further, the value after 2 months of exposure was comparable to that at 1 month of exposure, suggesting an adaptive response of cells which may exclude or expel TiO_2-NPs. This was confirmed by ICP-MS measurement of Ti accumulation in these cells, which also shows no statistically significant increase of intracellular Ti between 1 and 2 months of exposure (Table S1).

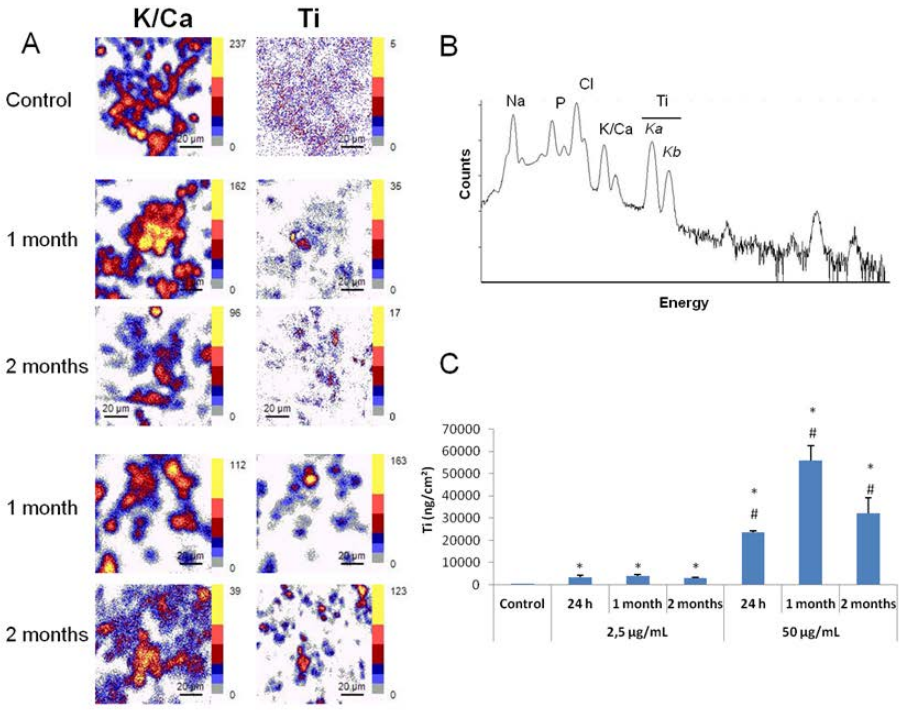

Figure 1. NP intracellular accumulation measured by µPIXE. Distribution maps of calcium and potassium (K/Ca, used as indicator of cell outlines) and titanium (Ti) together with their colour scale (counts): the hotter the color, the higher the concentration (A). Cells were analyzed after exposure to 0, 2.5 and 50 µg/mL NPs for 1 and 2 months. PIXE spectra displaying the regions of interest selected for mapping and quantification of Ti content in cells (B). Titanium concentration (ng/cm²) obtained by integration of PIXE spectra recorded on unexposed cells and cells exposed at 2.5 or 50 µg/mL for either 24 h, 1 month or 2 months (C). Results are presented as the mean of 8 points ± SEM. *: $p<0.05$ vs control cells; #: $p<0.05$ vs 2.5 µg/mL NP exposed cells.

At the sub-cellular level, TEM observation of cells exposed for 2 months to 2.5 and 50 µg/mL TiO_2-NPs showed that NPs were accumulated inside the cells under both conditions, mostly in cytoplasmic vacuole-like compartments which may be lysosomes or autophagosomes. No NP was observed in the nucleus or mitochondria (Figure 2).

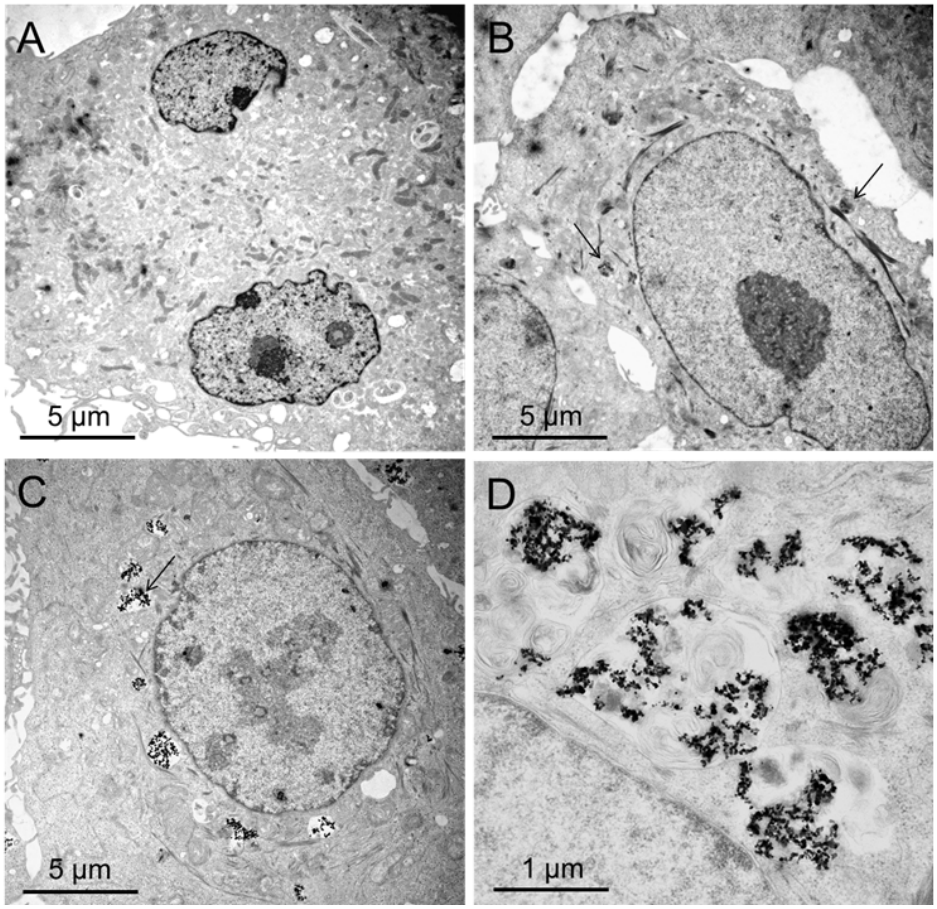

Figure 2. TEM images of A549 cells exposed to TiO_2-NPs. (A) Control cells (unexposed cells); (B) Cells exposed to 2.5 µg/mL NPs for 2 months; (C) and (D) Cells exposed to 50 µg/mL NP for 2 months.

No major accumulation of NPs was observed on cell membranes, confirming that the µPIXE and ICP-MS measurements reflected NP accumulation inside the cells rather than NPs adsorbed on cell membranes.

Cytotoxicity and cell proliferation

The MTT assay, assessing cell mitochondrial activity, demonstrated that chronic exposure to NPs did not affect cell survival, even after 2 months of exposure and at concentrations as high as 50 µg/mL TiO_2-NPs

(Figure 3A). Interference of NPs with the assay was tested using a previously reported protocol (Brun, 2014) and turned out to be negative (data not shown). This result was confirmed by trypan blue staining and cell counting at each cell passage, that revealed no overt mortality (Table S2), as well as propidium iodide staining and flow cytometry analysis of live/dead cells (Figure 3B), that also did not reveal any overt mortality.

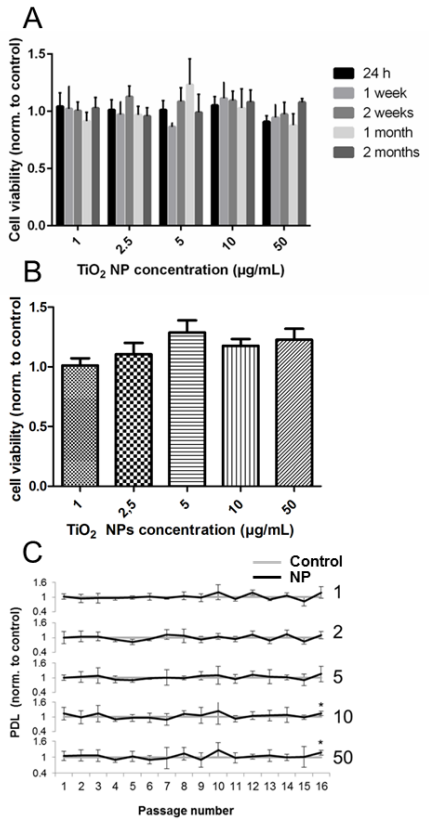

Figure 3. Cell viability after NP exposure. (A) Cellular metabolic activity, represented by the MTT assay; (B) cell viability, evaluated by propidium iodide staining; (C) Population doubling level (PDL), indicative of cell proliferation. Results are presented as the mean of 4 points ± SEM. *: $p<0.05$ vs control.

However, the population doubling level (PDL), inversely correlated to cell proliferation, was moderately but significantly increased for the 10 and 50 µg/mL TiO_2-NP exposure concentration and for the last passage (Figure 3C). This indicates that the highest exposure concentrations and the longest exposure time, even if non cytotoxic, significantly decreased cell proliferation.

Cellular redox status

As oxidative stress is both a known consequence of NP exposure and a demonstrated mechanism for genotoxicity, we evaluated the oxidative status of NP-exposed cells. ROS production, measured with the H_2DCFH-DA assay, was higher in cells exposed to 5, 10 and 50 µg/mL TiO_2-NPs than in control cells whatever the exposure time, as well as in cells exposed to 2.5 µg/mL TiO_2-NPs for 2 weeks and more (Figure 4). Increased intracellular ROS content was concentration-dependent, i.e. ROS content in cells exposed to 50 µg/mL TiO_2-NPs was significantly higher than in cells exposed to 5 and 10 µg/mL TiO_2-NPs. For our exposure condition we evaluated the interference of TiO_2-NPs with the assay as suggested by Guadagnini et al (Guadagnini, 2015); it did not account for more than 10% of the total DCF fluorescence even at the highest concentration, i.e. interference was not significant.

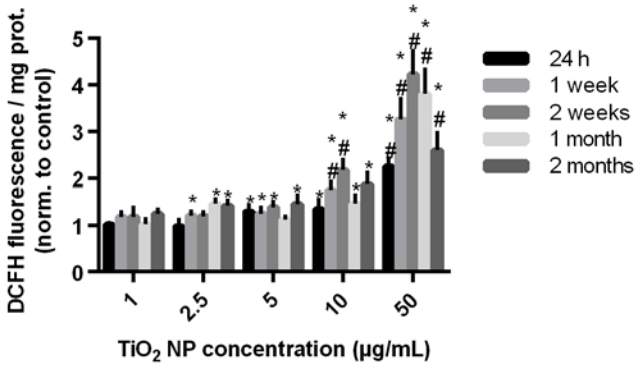

Figure 4. Intracellular ROS content after TiO_2-NP exposure. DCF fluorescence was normalized with respect to protein content, reflecting cell number. The obtained data were then normalized to untreated control. Value for positive control: H_2O_2 50 µM, 30 min: 2.1±0.3. Results are presented as the mean of 4 points ± SEM. *: $p<0.05$ vs control; #: $p<0.05$ vs lower dose for similar exposure period.

We did not observe any significant modulation of both total (GSH+GSSG) and reduced (GSSG) glutathione contents in cells continuously exposed to TiO_2-NPs for 2 months (Table S3). Neither did we observe any modulation of the activity of glutathione peroxidase (GPx) and glutathione reductase (GR) which are responsible for glutathione cycling between its reduced and oxidized form. The activity of superoxide dismutase (SOD) and catalase (CAT), involved in hydrogen peroxide and oxygen superoxide radical dismutation, respectively, were also unchanged after 2 months of exposure (Table S3). Finally, we

monitored mRNA expression of CAT, SOD1, SOD2, GPx1, GPx4 and GSR and observed no modulation of their expression (Table S4).

Genotoxicity

DNA damage was first evaluated via the alkaline version of the comet assay, which detects primary lesions of DNA i.e. single-strand breaks and double-strand breaks, as well as alkali-labile sites such as abasic sites. This assay showed increased DNA damage in cells exposed to 10 µg/mL TiO_2-NPs for 1 and 2 months, as well as in cells exposed to 50 µg/mL TiO_2-NPs regardless of the exposure time (Figure 5A). After 1 and 2 months of exposure, DNA damage was higher in cells exposed to 50 µg/mL TiO_2-NPs than in cells exposed to 10 µg/mL TiO_2-NPs.

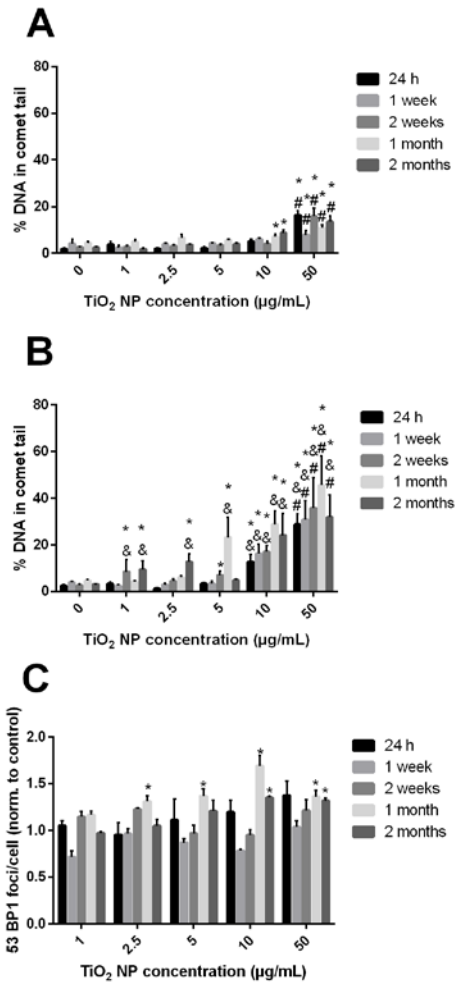

Figure 5: TiO_2-NP genotoxicity. (A) Alkaline comet assay, assessing single and double strand breaks as well as alkali-labile sites. Value for positive control: 50 µM H_2O_2 deposited on the slide 5 min before migration: 61.9%; (B) Fpg-modified comet assay, assessing single and double strand breaks, alkali-labile sites and oxidized bases. Value for positive control: riboflavin/UVA: 22.6%. Results are presented as the mean of % DNA in comet tail ± SEM (n=4). *: $p<0.05$ vs control; #: $p<0.05$ vs alkaline comet assay equivalent condition; $: $p<0.05$ vs lower dose for equivalent exposure period. (C) 53BP1 foci counting, assessing double strand DNA breaks. Total 53BP1 foci per image was reported relative to total cell number, and normalized to control data. Results are presented as the mean of 15 images ± SEM. *: $p<0.05$ vs control (unexposed cells). Value for controls: unexposed cells 0.27%, 25 µM etoposide: 1.95%.

We also used the -Fpg version of the comet assay, which additionally reveals Fpg sensitive sites, i.e. oxidative damage to DNA. In accordance with the recommendation of the European Standards Committee on Oxidative DNA damage (ESCODD) reported by Moller *et al.* (Moller, 2015) the number of Fpg-sensitive sites was very low in cells that were not exposed to TiO_2-NPs. Our positive control for this assay (cells not exposed to TiO_2-NPs, incubated for 30 min with riboflavin and exposed to UVA) resulted in 30-35% DNA in the tail, depending on the experiment (not shown). In this assay we observed higher % DNA in the comet tail than in the alkaline version of the assay, proving that exposure to TiO_2-NPs also caused oxidative damage to DNA. In Comet-Fpg, we observed a significant increase of DNA damage in cells exposed to 10 and 50 µg/mL TiO_2-NPs whatever the exposure time, as well as in cells exposed for 2 months at 1 µg/mL and 2.5 µg/mL TiO_2-NPs, and for 2 weeks and 1 month at 5 µg/mL TiO_2-NP (Figure 5B). Damage was higher in cells exposed to 50 µg/mL TiO_2-NP than in cells exposed to any other concentration of NPs, confirming the concentration-dependence of DNA damage.

We also measured the specific presence of DSB or DNA replication fork blockade by counting 53BP1 foci in the nuclei of cells chronically exposed to TiO_2-NPs. We observed higher 53BP1 foci counts in cells exposed to 2.5 and 5 µg/mL NPs during 1 month, and in cells exposed to 10 and 50 µg/mL NPs for 1 and 2 months (Figure 5C).

Finally, in order to evaluate clastogenic and aneugenic effects of NPs we used the cytokinesis-blocked micronucleus assay. Due to the possibility that cytochalasin B blocked endocytosis and consequently NP cellular uptake, we used the modified version of the assay where cells are incubated with NPs before being treated with cytochalasin B (Magdolenova, 2012). The percentage of binucleated cells, after 28 h of

exposure to cytochalasin B of cells chronically exposed to TiO_2-NPs, ranged between 55 and 65% and was not statistically different in control cells, as compared to TiO_2-NP-exposed cells. In binucleated cells, micronucleus counting did not reveal any chromosomal damage (Table S5). Moreover our positive control (100 µM of MMS for 24 h) significantly increased the number of micronuclei per binucleated cell (30.9±0.1 micronuclei per 1000 cells in cells exposed to MMS vs. 7.3±2.5 micronuclei per 1000 cells in unexposed cells, see Table S5). This proves that the mutagenicity and clastogenicity of TiO_2-NPs, under this exposure condition (i.e. chronic low level exposure, 1-50 µg/mL over 2 months), was insignificant.

Cell sensitization to post-exposure to a genotoxic agent

We previously showed that acute exposure to TiO_2-NPs impaired cellular ability to repair DNA lesions via NER and BER pathways (Jugan, 2012). Chronic exposure to TiO_2-NPs may thus sensitize cells to other genotoxic agents, particularly those which induce lesions that are classically repaired by the NER and the BER. We thus evaluated the impact of post-exposure to the alkylating agent methane-methyl sulfonate (MMS), which generates DNA lesions repaired by the BER, on cells continuously exposed to TiO_2-NPs for 2 months. First, these cells were exposed to a non-lethal concentration of MMS, i.e. 100 µM for 24 h. The MTT assay then demonstrated that cell mortality was higher in cells continuously exposed to 5 to 50 µg/mL NPs and subsequently acutely exposed to MMS, as compared to cells exposed to MMS without previous chronic exposure to NPs (Figure 6A). In order to confirm that this higher cell mortality was related to higher DNA damage, we quantified DNA strand break in cells chronically exposed to TiO_2-NPs and then acutely exposed to 50 µM or 100 µM of MMS. Post-exposure to 50 µM MMS did not increase the % tail DNA in alkaline comet assay (not shown). Conversely % tail DNA was increased by 14% in cells exposed to 50 µg/mL TiO_2-NPs for 2 months then post-exposed to 100 µM of MMS for 24 h, as compared to cells that were only exposed for 24 h to MMS (Figure 6B, grey bars). As a comparison, 2 months of exposure to 50 µg/mL TiO_2-NPs increased % tail DNA by 4%, as compared to unexposed cells (Figure 6B, white bars).

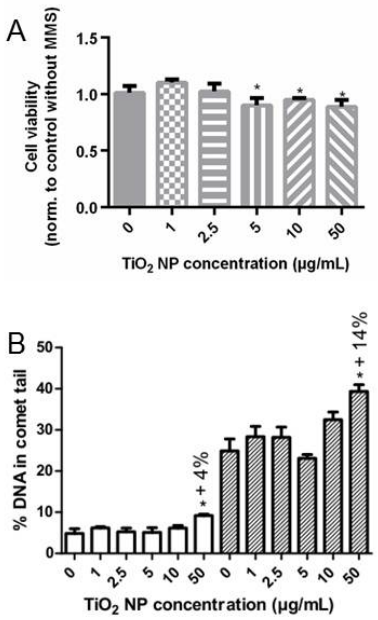

Figure 6: Cell sensitization to MMS due to long-term exposure to TiO_2-NPs. (A) Viability and (B) DNA strand breaks in cells exposed to NPs for 2 months and then to 100 µM MMS for 24h were assessed by MTT and alkaline comet assay, respectively. (A) Data were normalized to the results obtained in control cells, i.e. cells that were not exposed to MMS. Results are presented as the average of 6 points ± SEM. *: $p<0.05$ vs control (unexposed cells). (B) Results from alkaline comet assay, from cells exposed to TiO_2-NPs for 2 months (white bars) or to TiO_2-NPs for two months, then to 100 µM MMS for 24 h (grey bars). Data are expressed as % tail DNA and are the average of 3 comet slides (50 comets per slides) ± SEM. *: $p<0.05$ vs control (unexposed cells); the % indicates % increase as compared to control (unexposed) cells. Value for positive control: 50 µM H_2O_2 deposited on the slide 5 min before migration: 64.3%.

In addition, 53BP1 foci were counted in cells exposed to TiO_2-NPs for 2 months, then post-exposed to 50 µM or 100 µM of MMS. No statistically significant difference was observed in this assay (Figure S3). Finally we analyzed the mRNA expression of genes encoding proteins involved in DNA repair processes, especially via the BER pathway, i.e. APE1, PARP1, PCNA, XRCC1, POLB, LIG3, as well as genes encoding TP53 and the proteins involved in cell cycle checkpoint ATM and ATR, in cells chronically exposed to TiO_2-NPs. Their expression was not modified in cells exposed for 2 weeks, 1 month or 2 months to 2.5, 10 or 50 µg/mL TiO_2-NPs (Table S6). This indicates that if cells are sensitized to MMS

through reduction of their DNA repair capacities, as suggested by our previous results obtained after acute exposure to these TiO_2-NPs, this does not rely on the inhibition of expression of genes encoding DNA repair proteins.

Discussion

In the present article, we report the impact of long-term exposure of A549 lung cells to TiO_2-NPs, particularly focusing on the genome instability that it may provide. Our previously published results show that this exposure scenario induces DNA damage response via activation of the p53 pathway, through increased levels of STRAP which is a stabilizer of the coactivators of p53, p300 and JMY (Armand, 2015). We also showed that p53 acetylation and phosphorylation levels are increased (Armand, 2015). In the present article we complement these data by showing that this exposure scenario causes the accumulation of reactive oxygen species, oxidative damage to DNA, as well as the formation of foci of 53BP1 on the DNA which suggestss the presence of double-strand breaks and/or DNA repair processes by excision/synthesis and/or replication fork blockade. These lesions to DNA may be the cause of the p53 pathway activation that we previously reported. In this previous study, we also report that chronic exposure induced mitochondrial damage and perturbation of autophagy (Armand, 2015), which may be an explanation for the accumulation of ROS that we observe here. Indeed mitochondria and cellular respiration are the main source of endogenous ROS in mammalian cells. If these ROS are not appropriately scavenged, or if, as a result of mitochondrial damage, higher levels of ROS are produced, then these ROS would attack biomolecules including DNA. As discussed in our previous article (Jugan, 2012), oxidative damage to DNA may be created by weak oxidizing species such as hydroperoxides. These species may be produced in the cell cytoplasmic vacuole-like structures where TiO_2-NP accumulate, then migrate to the nucleus where they would oxidize DNA. Conversely the lifetime of OH°, the only ROS which is able to attack DNA backbone and create strand breaks (Pogozelski, 1998), is very short. Consequently, its migration from the cytoplasm/vacuoles to the nucleus, leading to direct DNA backbone attack, is improbable. The accumulation of 53BP1 foci that we observe might thus reflect the presence of double-strand breaks that result from secondary, indirect production of OH° in the nucleus.

Alternatively, and more probably, it may result from the repair of oxidative lesions by excision-synthesis processes, or replication fork blockade during mitosis due to damaged DNA (Bekker-Jensen, 2010). This hypothesis is further suggested by the low number of 53BP1 foci that we observe: in control cells we counted 0.2-0.3 53BP1 foci per cell nucleus while in cells exposed for 1 month to 2.5, 5 or 10 µg/mL TiO_2-NPs we observe 0.5 to 0.7 foci per cell nucleus. If secondary production of OH° in the nucleus was the cause of DNA backbone attack and 53BP1 foci formation, then this number would certainly be higher. Moreover, since we did not detect any micronuclei, it appears that these DNA strand breaks are efficiently repaired.

Our results are in line with the generally accepted paradigm that oxidative mechanisms drive TiO_2-NP toxicity, which is widely accepted for acute exposure mode (Johnston, 2009; Shi, 2013). It confirms the conclusion of the IARC Working Group, i.e. in vitro studies show that titanium dioxide particles, both fine and ultrafine, induce DNA damage that is "suggestive of the generation of reactive oxygen species" (IARC, 2010). Finally, it confirms that ROS accumulation is one of the earliest events occurring in cells chronically exposed to TiO_2-NP, as already reported (Huang, 2009; Wang, 2011) and that this ROS accumulation may result from mitochondrial impairment, or altered elimination of damaged mitochondria due to autophagy impairment as we previously reported (Armand, 2015). We also confirm here that 2 months exposure to TiO_2-NPs causes decreased cell proliferation, which was also hinted in our previous study where we reported cell cycle slowdown with cell accumulation in the G1 phase due to activation of the p53 pathway (Armand, 2015). Such perturbation of the cell cycle has also previously been reported by others upon acute (Wu, 2010) or long-term (Wang, 2011) exposure to TiO_2-NPs.

We show that TiO_2-NPs accumulate in cells where they distribute in cytoplasmic vesicles. Their accumulation kinetics suggest cellular adaptation to NP exposure, since Ti intracellular content after 2 months of continuous exposure is not statistically higher than after 1 month of exposure. This observation is in line with the results of Wang *et al.,* who observed significant decrease of Ti content in 60-day exposed cells, as compared to 2-day exposed cells (Wang, 2011). This adaptation could either be expulsion of NPs from the cells, for instance by activation of the exocytosis of NP-containing vesicles, or exclusion, i.e. reduced accumulation while dividing cells also divide their Ti content between daughter cells. It was recently demonstrated that NPs are not exported out of cells, and that NP accumulation

depends on the phase of the cell cycle, with more efficient uptake in G2/M phase than in S phase than in G0/G1 phase (Aberg, 2013; Kim, 2011). The cell cycle slowdown and cell accumulation in G1 phase thus supports the hypothesis of reduced intracellular accumulation rather than expulsion of TiO_2-NP from chronically-exposed cells.

Taken together, all these data can be summarized as follows:

Chronic exposure to TiO_2-NPs leads to their accumulation in cell cytoplasmic vesicles. Cells react to these exogenous compounds by activating autophagy, which fails to eliminate TiO_2-NPs. Autophagosomes then accumulate in cells, but no longer fulfil their role and do not eliminate altered mitochondria. Altered mitochondria accumulate in the cell cytoplasm, leading to increased release of ROS which induces oxidatively-generated DNA lesions. These lesions accumulate, together with strand breaks due to excision/resynthesis DNA repair processes and the replication fork blockade that they cause. Moreover the p53 pathway is activated by this mild stress, and leads to cell cycle slowdown and consequently decreased cell proliferation and decreased intracellular accumulation of TiO_2-NPs.

Another important issue highlighted in this study is that cells chronically exposed to TiO_2-NPs for 2 months are sensitized to the alkylating agent MMS, which is classically used as a positive control in genotoxicity experiments (Beranek, 1990). Indeed we observe MMS cytotoxicity when cells chronically exposed to TiO_2-NPs are then incubated with a sublethal dose of this alkylating agent, as well as increased levels of DNA strand breaks compared to the chronic controls (not exposed to MMS). This sensitization might be explained by two hypotheses. First, the DNA damage that we observed in our model can enhance the MMS-induced DNA damage to saturate DNA repair activity, leading to cell death. Second, TiO_2-NPs themselves can also impair cellular DNA repair activity, as we previously demonstrated upon acute exposure (Jugan, 2012). This observation underlines the need to deeply investigate the combined effects of NPs with other pollutants, particularly genotoxic compounds and alkylating agents.

Finally, our results show more drastic impacts from P25 TiO_2-NPs upon chronic exposure of A549 cells, particularly after 4 weeks of exposure, than those previously reported in the study of Vales et al. (Vales, 2014). This discrepancy may be due to the different cell lines that we used, BEAS-2B being bronchial cells while A549 are alveolar cells. Indeed alveolar cells, particularly A549 cells, produce and secrete pulmonary surfactant (Lieber, 1976), which changes the biochemical environment of the milieu around

these cells and may be adsorbed on the surface of NPs, changing their properties. Another explanation lies in the fact that different NPs were used in these two studies: we used P25 NPs, which are mixed anatase-rutile crystal phase and which generate a highly stable suspension in water and in cell culture medium. Conversely, Vales et al. (2014) used NMP102 TiO_2-NPs which are pure anatase and very hard to disperse in aqueous medium. For their experiments, these NPs were dispersed in BSA before being diluted in cell culture medium. This probably leads to the formation of a dense protein corona on the surface of these NPs. This corona may be different from the one that forms on the NPs used in our study, which were first dispersed in water then diluted in FBS-containing cell culture medium then exposed to the surfactant secreted by A549 cells. Since the protein corona on the surface of NPs plays a role in their cellular accumulation and impact (Monopoli, 2012), and since direct comparison shows that TiO_2-NPs dispersed either in BSA or in water lead to non-genotoxic or genotoxic impact, respectively (Magdolenova, 2012), these different NPs and dispersion protocols may explain the different toxicological outcomes observed.

Conclusions

We demonstrate here that long-term exposure to TiO_2-NPs (AEROXIDE® P25, Evonik; received as NM105 from the JRC) induces DNA damage in A549 cells and sensitizes these cells, ~~to post-exposure~~ as evidenced by the increased amount of DNA strand breaks induced by the alkylating agent MMS. Although this long-term exposure model is still far from the reality of human inhalation exposure, some genotoxicity endpoints appear positive even at very low exposure concentrations (as low as 1 µg/mL) ~~that we used~~. Chronic exposure causes more severe DNA damage than acute exposure, particularly those revealed by 53BP1 foci immunostaining, i.e. double-strand breaks or replication fork blockade ~~double-strand breaks~~. This underlines the necessity to use chronic exposure scenarios in addition to acute exposure models in order to investigate NP impact, since these distinct models lead to different adverse outcomes, with additional triggering events and more intense effects in long-term exposure scenarios.

Acknowledgement

This work was funded by CEA through the Nanoscience and Toxicology research programs, and via the European Commission's 7th Framework Programme project NanoMILE (Contract No. NMP4-LA-2013-310451). It is a contribution to the Labex Serenade (n° ANR-11-LABX-0064) funded by the "Investissements d'Avenir" French Government program of the French National Research Agency (ANR) through the A*MIDEX project (n° ANR-11-IDEX-0001-02). This research received support from the QualityNano Project http://www.qualitynano.eu which is financed by the European Community Research Infrastructures under the FP7 Capacities Programme (Grant No. INFRA-2010-262163), and its partner University of Birmingham. The authors would like to thank Veronique Collin-Faure for flow cytometry analyses.

Declaration of interest

The authors declare that there are none.

References

Aberg C, Kim JA, Salvati A, Dawson KA. 2013. Theoretical framework for nanoparticle uptake and accumulation kinetics in dividing cell populations. Epl 101(3).

Armand L, Biola-Clier M, Bobyk L, Collin-Faure V, Diemer H, Strub J-M, Cianferani S, Van Dorsselaer A, Herlin-Boime N, Rabilloud T, Carriere M. 2015. Molecular responses of alveaolar epithelial A549 cells to chronic exposure to titanium dioxide nanoparticles: a proteomic view. Journal of Proteomics in press.

Baan RA. 2007. Carcinogenic hazards from inhaled carbon black, titanium dioxide, and talc not containing asbestos or asbestiform fibers: Recent evaluations by an IARC Monographs working group. Inhalation Toxicology 19: 213-228.

Barberet P, Incerti S, Andersson F, Delalee F, Serani L, Moretto P. 2009. Technical description of the CENBG nanobeam line. Nuclear Instruments & Methods in Physics Research Section B-Beam Interactions with Materials and Atoms 267(12-13): 2003-2007.

Barillet S, Jugan ML, Laye M, Leconte Y, Herlin-Boime N, Reynaud C, Carriere M. 2010. In vitro evaluation of SiC nanoparticles impact on A549 pulmonary cells: Cyto-, genotoxicity and oxidative stress. Toxicology Letters 198(3): 324-330.

Bekker-Jensen S, Mailand N. 2010. Assembly and function of DNA double-strand break repair foci in mammalian cells. DNA Repair 9(12): 1219-28.

Beranek DT. 1990. Distribution of methyl and ethyl adducts following alkylation with monofunctional alkylating-agents. Mutation Research 231(1): 11-30.

Brun E, Barreau F, Veronesi G, Fayard B, Sorieul S, Chaneac C, Carapito C, Rabilloud T, Mabondzo A, Herlin-Boime N, Carriere M. 2014. Titanium dioxide nanoparticle impact and translocation through ex vivo, in vivo and in vitro gut epithelia. Particle and Fibre Toxicology 11.

Campbell JL, Boyd NI, Grassi N, Bonnick P, Maxwell JA. 2010. The Guelph PIXE software package IV. Nuclear Instruments & Methods in Physics Research Section B-Beam Interactions with Materials and Atoms 268(20): 3356-3363.

Carriere M, Gouget B, Gallien JP, Avoscan L, Gobin R, Verbavatz JM, Khodja H. 2005. Cellular distribution of uranium after acute exposure of renal epithelial cells: SEM, TEM and nuclear

microscopy analysis. Nuclear Instruments & Methods in Physics Research Section B-Beam Interactions with Materials and Atoms 231: 268-273.

Carriere M, Pigeot-Remy S, Casanova A, Dhawan A, Lazzaroni J-C, Guillard C, Herlin-Boime N. 2014. Impact of titanium dioxide nanoparticle dispersion state and dispersion method on their toxicity towards A549 lung cells and Escherichia coli bacteria. Journal of translational toxicology 1: 10-20.

Chen T, Yan J, Li Y. 2014. Genotoxicity of titanium dioxide nanoparticles. Journal of Food and Drug Analysis 22(1): 95-104.

Collins AR. 2009. Investigating Oxidative DNA damage and its repair using the comet assay. Mutation Research-Reviews in Mutation Research 681(1): 24-32.

Fenech M. 2000. The in vitro micronucleus technique. Mutation Research-Fundamental and Molecular Mechanisms of Mutagenesis 455(1-2): 81-95.

Gerloff K, Albrecht C, Boots AW, Forster I, Schins RP. 2009. Cytotoxicity and oxidative DNA damage by nanoparticles in human intestinal Caco-2 cells. Nanotoxicology 3(4): 355-364.

Guadagnini R, Halamoda Kenzaoui B, Walker L, Pojana G, Magdolenova Z, Bilanicova D, Saunders M, Juillerat-Jeanneret L, Marcomini A, Huk A, Dusinska M, Fjellsbo LM, Marano F, Boland S. 2015. Toxicity screenings of nanomaterials: challenges due to interference with assay processes and components of classic in vitro tests. Nanotoxicology 1: 13-24.

Gurr JR, Wang ASS, Chen CH, Jan KY. 2005. Ultrafine titanium dioxide particles in the absence of photoactivation can induce oxidative damage to human bronchial epithelial cells. Toxicology 213(1-2): 66-73.

Hackenberg S, Scherzed A, Technau A, Froelich K, Hagen R, Kleinsasser N. 2013. Functional Responses of Human Adipose Tissue-Derived Mesenchymal Stem Cells to Metal Oxide Nanoparticles In Vitro. Journal of Biomedical Nanotechnology 9(1): 86-95.

Huang S, Chueh PJ, Lin Y-W, Shih T-S, Chuang S-M. 2009. Disturbed mitotic progression and genome segregation are involved in cell transformation mediated by nano-TiO2 long-term exposure. Toxicology and Applied Pharmacology 241(2): 182-194.

IARC. 2010. Carbon black, titanium dioxide, and talc. IARC Monogr Eval Carcinog Risks Hum 93: 1-413.

Johnston HJ, Hutchison GR, Christensen FM, Peters S, Hankin S, Stone V. 2009. Identification of the mechanisms that drive the toxicity of TiO(2)particulates: the contribution of physicochemical characteristics. Part Fibre Toxicol 6(33): 1743-8977.

Jugan M-L, Barillet S, Simon-Deckers A, Herlin-Boime N, Sauvaigo S, Douki T, Carriere M. 2012. Titanium dioxide nanoparticles exhibit genotoxicity and impair DNA repair activity in A549 cells. Nanotoxicology 6(5): 501-513.

Kim JA, Aberg C, Salvati A, Dawson KA. 2011. Role of cell cycle on the cellular uptake and dilution of nanoparticles in a cell population. Nat Nanotechnol 7(1): 62-8.

Kocbek P, Teskac K, Kreft ME, Kristl J. 2010. Toxicological Aspects of Long-Term Treatment of Keratinocytes with ZnO and TiO2 Nanoparticles. Small 6(17): 1908-1917.

Lieber M, Smith B, Szakal A, Nelson-Rees W, Todaro G. 1976. A continuous tumor-cell line from a human lung carcinoma with properties of type II alveolar epithelial cells. Int J Cancer 17(1): 62-70.

Loomis D, Grosse Y, Lauby-Secretan B, El Ghissassi F, Bouvard V, Benbrahim-Tallaa L, Guha N, Baan R, Mattock H, Straif K, Iarc. 2013. The carcinogenicity of outdoor air pollution. Lancet Oncology 14(13): 1262-1263.

Magdolenova Z, Bilanicova D, Pojana G, Fjellsbo LM, Hudecova A, Hasplova K, Marcomini A, Dusinska M. 2012. Impact of agglomeration and different dispersions of titanium dioxide nanoparticles on the human related in vitro cytotoxicity and genotoxicity. J Environ Monit 14(2): 455-64.

Magdolenova Z, Lorenzo Y, Collins A, Dusinska M. 2012. Can standard genotoxicity tests be applied to nanoparticles? J Toxicol Environ Health A 75(13-15): 800-6.

Mayer M. 2002. Ion beam analysis of rough thin films. Nuclear Instruments & Methods in Physics Research Section B-Beam Interactions with Materials and Atoms 194(2): 177-186.

Moller P, Jensen DM, Christophersen DV, Kermanizadeh A, Jacobsen NR, Hemmingsen JG, Danielsen PH, Karottki DG, Roursgaard M, Cao Y, Jantzen K, Klingberg H, Hersoug LG, Loft S. 2015. Measurement of oxidative damage to DNA in nanomaterial exposed cells and animals. Environ Mol Mutagen 56(2): 97-110.

Monopoli MP, Aberg C, Salvati A, Dawson KA. 2012. Biomolecular coronas provide the biological identity of nanosized materials. Nat Nanotechnol 7(12): 779-86.

Paur H-R, Cassee FR, Teeguarden J, Fissan H, Diabate S, Aufderheide M, Kreyling WG, Hanninen O, Kasper G, Riediker M, Rothen-Rutishauser B, Schmid O. 2011. In-vitro cell exposure studies for the assessment of nanoparticle toxicity in the lung-A dialog between aerosol science and biology. Journal of Aerosol Science 42(10): 668-692.

Pogozelski WK, Tullius TD. 1998. Oxidative Strand Scission of Nucleic Acids: Routes Initiated by Hydrogen Abstraction from the Sugar Moiety. Chem Rev 98(3): 1089-1108.

Robichaud CO, Uyar AE, Darby MR, Zucker LG, Wiesner MR. 2009. Estimates of Upper Bounds and Trends in Nano-TiO2 Production As a Basis for Exposure Assessment. Environmental Science & Technology 43(12): 4227-4233.

Shi H, Magaye R, Castranova V, Zhao J. 2013. Titanium dioxide nanoparticles: a review of current toxicological data. Particle and Fibre Toxicology 10.

Simon-Deckers A, Gouget B, Mayne-L'Hermite M, Herlin-Boime N, Reynaud C, Carriere M. 2008. In vitro investigation of oxide nanoparticle and carbon nanotube toxicity and intracellular accumulation in A549 human pneumocytes. Toxicology 253(1-3): 137-146.

Singh NP, McCoy MT, Tice RR, Schneider EL. 1988. A simple technique for quantitation of low-levels of DNA damage in individual cells. Experimental Cell Research 175(1): 184-191.

Vales G, Rubio L, Marcos R. 2014. Long-term exposures to low doses of titanium dioxide nanoparticles induce cell transformation, but not genotoxic damage in BEAS-2B cells. Nanotoxicology 19: 1-11.

Wang S, Hunter LA, Arslan Z, Wilkerson MG, Wickliffe JK. 2011. Chronic Exposure to Nanosized, Anatase Titanium Dioxide Is Not Cyto- or Genotoxic to Chinese Hamster Ovary Cells. Environmental and Molecular Mutagenesis 52(8): 614-622.

Weir A, Westerhoff P, Fabricius L, Hristovski K, von Goetz N. 2012. Titanium Dioxide Nanoparticles in Food and Personal Care Products. Environmental Science & Technology 46(4): 2242-2250.

Wu J, Sun J, Xue Y. 2010. Involvement of JNK and P53 activation in G2/M cell cycle arrest and apoptosis induced by titanium dioxide nanoparticles in neuron cells. Toxicology Letters 199(3): 269-276.

Supplementary Material for:

Long-term exposure of A549 cells to titanium dioxide nanoparticles induces DNA damage and sensitizes cells towards genotoxic agents

Lucie Armand, Adeline Tarantini, David Beal, Mathilde Biola-Clier, Laure Bobyk, Sephanie Sorieul, Karin Pernet-Gallay, Caroline Desvergne, Iseult Lynch, Nathalie Herlin-Boime, Marie Carriere

Supplementary Material and Methods

- ICP-MS quantification of Ti accumulation in A549 cells chronically exposed to TiO_2-NPs

In order to confirm our µPIXE results, we also measured Ti accumulation in A549 cells using ICP-MS. Cells exposed for 24 h, 1 month or 2 months to 2.5, 10 or 50 µg/mL TiO_2-NPs, as well as untreated cells (controls) (4 replicates per condition), were rinsed four times with 150 mM NaCl in order to remove NPs that were bound to cell surface, then harvested in 50 µL of 150 mM NaCl and stored at -20°C until mineralization and analysis. This whole experiment was repeated twice. Prior to analysis using ICP-MS, all dispersion glassware were carefully cleaned and washed in 10% (v/v) HNO_3 and rinsed repeatedly with ultrapure water. Cells were dissolved by microwave-assisted decomposition in 10 mL of 48% (vol/vol) ultrapure H_2SO_4 for 30 min at 1100 W, as previously described (Dorier, 2015). Digested sample were stored in unused and sterilized 7 mL bijou tubes. Samples were then diluted in ultrapure 1% (vol/vol) HNO_3 and analyzed on an Agilent 7500ce ICP-MS equipped with a concentric nebulizer and operated in the helium collision mode for Ti (to eliminate interference from polyatomic species). They were introduced to the ICP-MS via the autodiliter (to avoid matrix effects). ^{47}Ti concentration was analyzed due to interference of S from H_2SO_4 on ^{48}Ti, using ^{45}Sc, ^{72}Ge, ^{115}In and ^{159}Tb as internal standards. Calibration standards (0 – 200 µg/l) were prepared from VWR 1000 mg/l stock solutions. The release of Ti ions from TiO_2-NP suspensions was monitored immediately after sonication and then 2 months after sonication. For this purpose, 500 µL of the 10 mg/mL water suspension was ultracentrifuged (400 000×*g*, 30 min), then Ti content was measured in the supernatant by ICP-MS; release of Ti ion was 0.036±0.001% of the initial Ti content in the 2 months-old suspension, showing that NP dissolution was not significant.

- Monitoring of glutathione content, superoxide dismutase, catalase, glutathione reductase and peroxidase activities

Cells lysates (3 replicates per condition) were prepared by scraping in phosphate buffer supplemented with glycerol and phenylmethanesulfonyl fluoride, frozen in liquid nitrogen then thawed at 37°C three times. They were then centrifuged (4 °C, 15 min, 10,000 g) and supernatants were collected, their protein concentration was measured and normalized, then samples were aliquoted and stored at -80°C until analysis. Glutathione intracellular content, either total (GSH+GSSG) or reduced (GSH) was determined as

previously described (Vandeputte et al., 1994). GSH content was measured via its oxidation by 5,5'-dithiobis(2-nitrobenzoic acid) (DTNB), which leads to the formation of 5-thio(2-nitrobenzoic acid) (TNB), a yellow by-product absorbing at 405 nm. The same protocol was applied for the determination of total glutathione content (GSH+GSSG), with a preliminary step of reduction of oxidized glutathione (GSSG) by glutathione reductase (GR). After addition of DTNB to cell lysates, absorbance at 405 nm was followed during 5 minutes. GSH and GSH+GSSG concentrations in cell lysates were then determined by comparison to GSH calibration curves.

GR activity was measured using an assay based on the oxidation of GSH by DTNB (Carlberg, 1985). Phosphate buffer to which was added 1 mM EDTA, 400 µM DTNB, 300 µM NADPH and 800 µM GSSG was applied to the cell lysate. Absorbance at 405 nm was then measured continuously for 5 min. GR activity was then calculated from a GR standard calibration curve. GPx activity was also determined spectrophotometrically, by coupling the oxidation of glutathione with NADPH using GR (Paglia, 1967). Cell lysates were mixed with phosphate buffer to which was added GSH, NADPH and GR. Then cumene hydroperoxide was added to this mixture in order to initiate the reaction, and absorbance was immediately measured at 340 nm. SOD activity was measured as an indirect assay in which β-mercaptoethanol competes with endogenous SOD for nicotinamide adenine dinucleotide (NADH) oxidation by $O_2^{\bullet -}$ (Paoletti, 1986). One unit of SOD activity is defined as the amount that causes 50% inhibition of NADH oxidation under specific conditions. Phosphate buffer supplemented with 350 µM NADH, 3mM EDTA, and 1.5 mM and MnCl2. 2-mercapto-ethanol (10 mM) was added to cell lysates. After a 20 min incubation period at room temperature, absorbance at 340 nm was read during 5 minutes. SOD activity was then determined by comparison with a SOD activity calibration curve. CAT activity was measured by spectrophotometrically monitoring the disappearance of exogenous H_2O_2 (Beers, 1952). Standard solutions of known CAT activities (0.5-50 U/mL) were prepared in phosphate buffer (100 mM, pH 7.8). H_2O_2 was added to cell lysate then absorbance was read at 240 nm for 5 minutes. Catalase activity was then deduced to CAT standard calibration curve.

- RT-qPCR analysis of the expression of genes involved in oxidative stress response and DNA repair

mRNA expression of genes encoding superoxide dismutase 1 and 2 (SOD1, SOD2), catalase (CAT), Glutathione peroxidase 1 and 4 (GPx1, GPx4), glutathione reductase (GSR), tumor protein p53 (TP53), ataxia telangiectasia mutated (ATM), ataxia telangiectasia and Rad3-related protein (ATR), apurinic/apyrimidic endonuclease (APE1), poly(ADP-ribose) polymerase 1 (PARP1), proliferating cell nuclear antigene (PCNA), X-ray repair cross-complementing protein 1 (XRCC1), polymerase β (POLB) and ligase 3 (LIG3) was evaluated by reverse-transcription quantitative polymerase chain reaction (RT-qPCR). RNA concentration and purity were assessed using a Nanodrop ND-1000 spectrophotometer (Thermo Fisher Scientific) by measuring absorbance at 230, 260 and 280 nm. For each exposure condition we used three biological replicates, deposited in technical duplicate on the qPCR plate. Glyceraldehyde-3-phosphate dehydrogenase (GAPDH) and cyclophilin B (CycloB) were chosen as reference genes for normalization and were validated using BestKeeper (Pfaffl, 2004). Primer sequences were: GAPDH, forward 5'-gagtcaacggatttggtcgt-3' reverse 5'-ttgattttggagggatctcg-3'; SOD1, forward 5'-agggcatcatcaatttcgag-3' reverse 5'-acattgcccaagtctccaac-3'; SOD2, forward 5'-tccactgcaaggaacaacag-3' reverse 5'-tcttgctgggatcattaggg-3'; CAT, forward 5'-agcttagcgttcatccgtgt-3' reverse 5'-tccaatcatccgtcaaaaca-3'; GPx1, forward 5'-ccagtcggtgtatgccttct-3' reverse 5'-ctcttcgttcttggcgttct-3'; GPx4, forward 5'-tcagcaagatctgcgtgaac-3' reverse 5'-ggggcaggtccttctctatc-3'; GSR, forward 5'-gatcccaagcccacaataga-3' reverse 5'-cttagaacccagggctgaca-3'; TP53, forward 5'-gttccgagagctgaatgagg-3' reverse 5'-tctgagtcaggcccttctgt-3'; ATM, forward 5'-ggacagtggaggcacaaaat-3' reverse 5'-gtgtcgaagacagctggtga-3'; ATR, forward 5'-ctcgctgaactgtacgtgga-3' reverse 5'-gcatagctcgaccatggatt-3'; APE1, 5'-gctgcctggactctctcatc-3' reverse 5'-gctgttaccagcacaaacga-3'; PARP1, forward 5'-gctcctgaacaatgcagaca-3' reverse 5'-cattgtgtgtggttgcatga-3'; PCNA, forward 5'-ggctctagcctgacaaatgc-3' reverse 5'-gcctccaacaccttcttgag-3'; XRCC1, forward 5'-cagccctacagcaaggactc-3' reverse 5'-gctgtgactggggatgtctt-3'; POLB, forward 5'-gagaagaacgtgagccaagc-3' reverse 5'-cgtatcatcctgccgaatct-3'; LIG3, forward 5'-gctcagcaggagatggtttc-3' reverse 5'-tctaggtcccgtgccatatc-3'). We used the following thermal cycling steps: 95°C for 5 min, then 95°C for 15 s, 55°C for 20 s and 72°C for 40 s 40 times and finally 95°C for 1 min, 55°C for 30 s and 95°C for 30 s for the dissociation curve, on an Mx3005P qPCR system (Stratagene) using MESA blue qPCR master mix for SYBR Assay Low ROX (Eurogentec). PCR efficiencies were experimentally checked for compliance using a mix of all samples, with a quality criterion

of 2 ± 0.3, and a theoretical value of 2 was used for calculations. Cq threshold was determined using the Mx-Pro 3.20 software (Stratagene) with default settings. mRNA expression analysis, normalization and statistical analysis were performed using the ΔΔCq method as described previously (Dorier, 2015).

Figure S1. Schematic representation of the exposure protocol. Each orange circle represents a 58 cm² petri dish of A549 cells in cell culture medium containing 0, 1, 2.5, 5, 10 or 50 µg/mL TiO_2-NPs. Arrows indicate that these petri dishes/cells are incubated/grown for 3 or 4 days at 37°C/5% CO_2, then passaged using trypsin and seeded in a new petri dish containing 0, 1, 2.5, 5, 10 or 50 µg/mL TiO_2-NPs (each new dish receives the same NP concentration as in the previous 3-4 days exposure period). Cells were counted after trypan blue staining at each cell passage. At the last passage before the 1 week, 2 weeks, 1 month and 2 months timepoints, 2 series of petri dishes were prepared, one for the continuation of the chronic exposure, and the other for sampling for the targeted experiments. For this latter series, cells were also seeded in NP-containing cell culture medium (same concentration as in the previous 3-4 days exposure period). Regarding the 24 h timepoint, one series of petri dishes began the chronic exposure, and series of cells were also directly seeded on the appropriate plate/petri dish/microscopy coverslip, in culture medium containing 0, 1, 2.5, 5, 10 or 50 µg/mL TiO_2-NPs, for performing the targeted experiment 24 h later. Samples for the targeted experiments included frozen cells, at each exposure concentration, for flow cytometry analysis of cell viability evaluation, ICP-MS measurement, glutathione and other redox enzyme activity measurement, comet assay and RT-qPCR analysis. They also included cell seeding on the appropriate plate/petri dish/microscopy coverslip in culture medium containing 0, 1, 2.5, 5, 10 or 50 µg/mL TiO_2-NPs, for MTT and H2DCF-DA assays, 53BP1, CBMN, µPIXE and TEM preparations, as well as for subsequent exposure to MMS for cell sensitization experiments. The whole experiment was repeated 4 times independently.

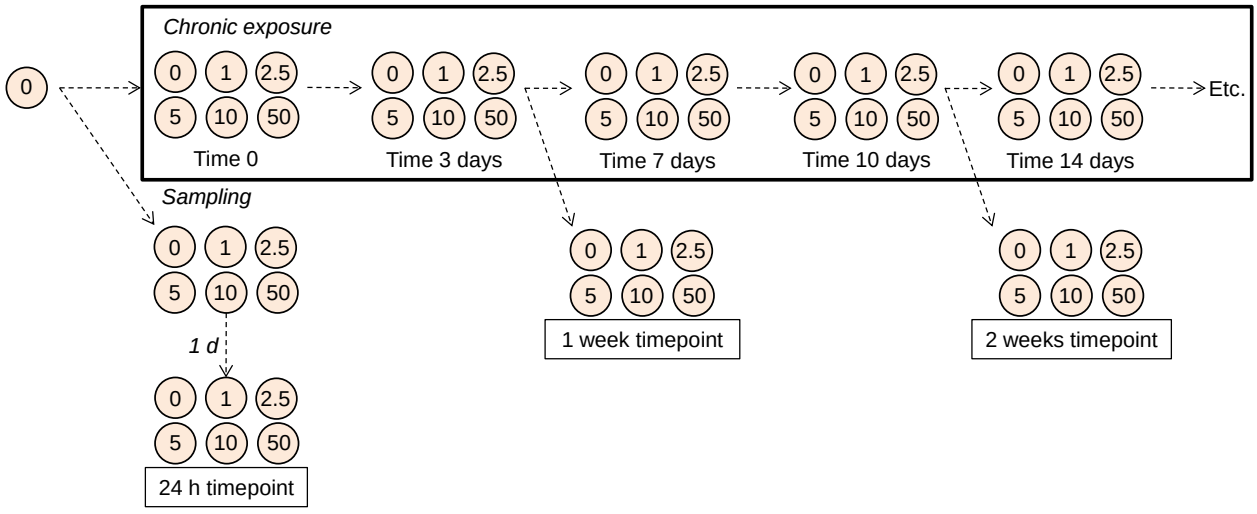

Figure S2. Nanoparticle size distribution. Histogram of NP size distribution 24 h after dispersion in ultrapure water at 10 µg/mL (black bars) or 24 h after dilution in filtered culture medium containing 10% FBS to a concentration of 40 µg/mL (grey bars) (A). TEM image of NP suspension after dispersion in water; scale bar 200 nm (B).

A

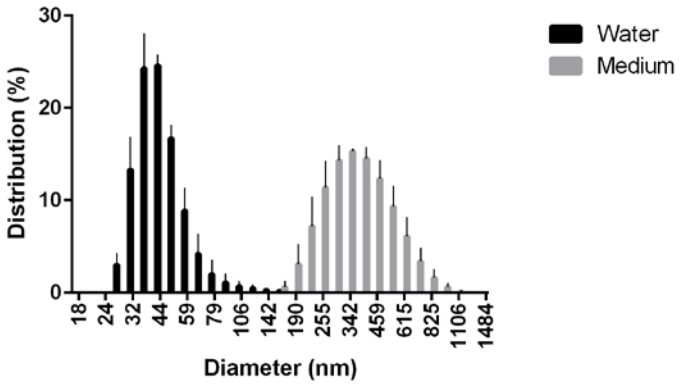

B

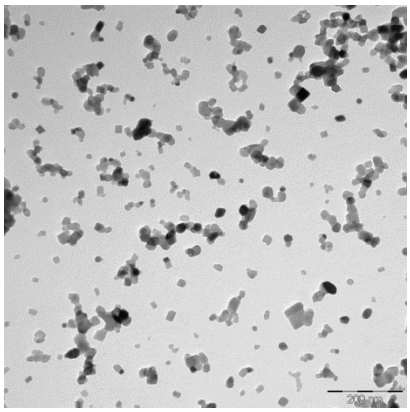

Figure S3. 53BP1 foci counting after long-term exposure to TiO_2-NPs and post-exposure to genotoxic agents. Cells were exposed to 1-50 µg/mL TiO_2-NPs for 2 months then post-exposed for 24 h to 50 or 100 µM of MMS (MMS 50 and MMS 100, respectively) or 5 or 10 µM of etoposide (Etoposide 5 and Etoposide 10, respectively). After immunostaining, the number of 53BP1 foci per cell nucleus was counted automatically using a CellInsight CX5 (Life Technologies). Results are average ± standard deviation of 53BP1 foci count per cell nucleus. *: $p<0.05$ vs. control (cells not exposed to TiO_2-NPs): differences were not statistically significant.

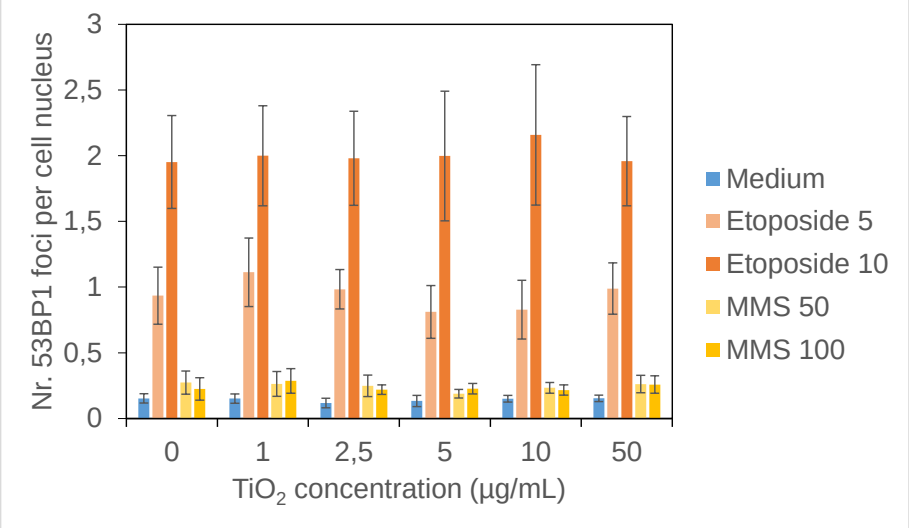

Table S1. Experimental conditions and replicates[a]

Assay	Nr. repl. per exp.	Nr. indep. exp.	Storage (Yes/no), condition	Expo. time	Expo. concentration (µg/mL)
TEM	1	1	Yes, fixed glutaraldehyde, RT	2 m.	0, 2.5, 50
µPIXE	1, 4 measurements	2	Yes, cryofixed, freeze-dried	24 h, 1 m., 2 m.	0, 2.5, 50
ICP-MS	4	1	Yes, -20°C	24 h, 1 m., 2 m.	0, 2.5, 50
MTT	6	4	No	all	all
Trypan blue	2	4	No	all	all
PI (FACS)	4	3	No	all	all
H2DCFDA	4	4	No	all	all
Redox enzymes	3	3	Yes, -80°C	all	all
Comet assay	1, 3 slides (alkaline) and 3 slides (-Fpg)	4	Yes, -80°C	all	all
53BP1	1, 15 images	4	Yes, fixed PFA, RT	all	all
Micronucleus	3, 20 images per slide	4	Yes, fixed PFA, RT	all	all
RT-qPCR	3	4	Yes, -80°C	all	all

[a]Abbreviations: Nr. repl. per exp.: number of replicate per experiment. Nr. indep. exp.: number of independent, 2 month exposure experiment on which this assay was carried out. Expo. time; expo. concentration: exposure time; exposure concentration. RT: room temperature. PFA: paraformaldehyde, 1 m.: 1 month, 2 m.: 2 months. Experimental details: for µPIXE we prepared one cell sample, and analyzed 4 different areas of this sample. For comet assay we prepared one cell sample that was stored frozen at -80°C and just before comet experiment this sample was defrosted and we prepared 3 comet slides for alkaline comet assay and 3 comet slides for Fpg-modified comet assay from this single sample.

Table S1. Ti accumulation in A549 cells, as measured by ICP-MS[a]

	2.5 µg/mL	10 µg/mL	50 µg/mL
24 h	22.7 ± 3.9	13.7 ± 0.6	95.6 ± 1.5
1 month	19.1±1.0	52.0 ± 12.2	119.4 ± 6.7*
2 months	16. ± 0.5*	74.0 ± 5.6*	97.5 ± 7.7*

[a]Measurement of Ti content in A549 cells exposed for 24 h, 1 month or 2 months to 2.5, 10 or 50 µg/mL TiO_2-NPs, further normalized with respect to protein concentration in the samples. Results are expressed as µg Ti per mg protein, measured on approximately 350 000 cells per condition. Mean of four replicates ± standard deviation. *: $p<0.05$ vs control (unexposed cells); #: $p<0.05$ 1 month vs 2 months: differences were not statistically significant.

Table S2. Cell viability by trypan blue staining

	TiO_2-NP concentration (µg/mL)					
	0	1	2.5	5	10	50
24 h	96%	95%	96%	99%	98%	96%
1 week	98%	99%	97%	99%	99%	99%
2 weeks	97%	98%	99%	99%	98%	99%
1 month	96%	96%	97%	98%	96%	96%
2 months	97%	97%	97%	98%	98%	97%

[a]Cells were trypsinized then diluted (vol./vol.) in trypan blue (Life Technologies). Live and dead cells were counted using a Countess automated cell counter (Life Technologies).

Table S3. Status of cellular anti-oxidative systems[a]

	TiO_2-NP concentration (µg/mL)				
	1	2.5	5	10	50
GSH+GSSG	1.11±0.13	0.96±0.11	1.30±0.15	1.13±0.10	1.26±0.12
GSH	1.00±0.11	1.06±0.12	1.00±0.10	1.02±0.10	1.01±0.07
GR	0.97±0.05	0.97±0.15	1.00±0.06	0.90±0.15	0.84±0.27
GPX	0.80±0.10	0.87±0.14	0.80±0.10	1.05±0.02	1.08±0.09
SOD	n/a	n/a	n/a	1,2±0.03	1.01±0.02
CAT	n/a	n/a	n/a	1,4±0.3	1.2±0.2

[a]Total (GSH+GSSG) and reduced (GSH) glutathione content, glutathione reductase (GR), glutathione peroxidase (GPX), superoxide dismutase (SOD) and catalase (CAT) activities in cells after 2 months of exposure to TiO_2-NPs, normalized to control (unexposed cells). n/a: not measured. Mean of four replicates ± standard error. *: $p<0.05$ vs control (unexposed cells): differences were not statistically significant.

Table S4. mRNA expression of genes involved in cellular redox balance[a]

Time	NP (µg/mL)	CAT	SOD1	SOD2	GSR	GPX4	GPX1
24 h	2.5	1.05±0.34	1.27±0.12	1.41±0.79	1.21±0.29	1.43±0.21	1.53±0.18
	10	1.53±0.55	1.72±0.47	1.93±0.78	1.42±0.40	1.34±0.30	1.49±0.26
	50	1.03±0.16	0.93±0.15	1.82±1.36	1.03±0.16	1.25±0.41	1.00±0.11
2 w.	2.5	1.20±0.45	1.38±0.37	1.02±0.80	1.18±0.16	1.56±0.44	1.32±0.40
	10	0.83±0.50	0.96±0.26	1.30±0.83	1.03±0.17	1.45±0.60	1.17±0.28
	50	0.68±0.16	0.66±0.07	1.49±1.06	0.90±0.19	1.37±0.36	1.15±0.51
1 m.	2.5	0.78±0.17	0.96±0.16	1.21±0.78	1.05±0.15	1.02±0.33	1.18±0.31
	10	0.80±0.28	0.90±0.21	0.90±0.43	0.90±0.37	1.20±0.55	1.29±0.16
	50	0.83±0.07	1.19±0.19	1.00±0.43	1.03±0.21	1.23±0.22	1.47±0.17
2 m.	2.5	0.98±0.12	1.30±0.16	1.22±0.95	1.09±0.25	0.84±0.11	1.09±0.54
	10	0.70±0.21	1.08±0.27	1.02±0.68	0.99±0.21	0.86±0.19	1.05±0.52
	50	0.82±0.17	1.05±0.24	1.12±0.79	0.92±0.08	0.80±0.09	1.13±0.61

[a]Gene expression was measured by RT-qPCR on A549 cells exposed for 24 h, 2 weeks (2 w.), 1 month (1 m.) or 2 months (2 m.) to 0, 2.5, 10 or 50 µg/mL TiO_2-NP. Results are expressed as $2^{-\Delta\Delta Cq}$ calculated with the reference gene GAPDH. Mean of four replicates ± standard error. *: $p<0.05$ vs control (unexposed cells): differences were not statistically significant.

Table S5. Cytokinesis-blocked micronucleus assay[a]

	TiO_2-NP concentration (µg/mL)					
	0	1	2.5	5	10	50
24 h	7.3±2.5	10.8±4.7	5.4±7.3	7.4±6.5	6.5±5.6	5.9±2.7
	(54.4±6.5)	(53.4±5.9)	(58.5±5.2)	(56.8±3.8)	(58.7±6.4)	(54.0±7.0)
1 week	4.9±4.5	4.9±5.2	3.5±6.0	4.0±3.7	6.9±6.7	8.2±7.9
	(52.9±17.9)	(51.1±16.2)	(56.6±10.5)	(54.3±14.6)	(56.3±12.4)	(54.0±17.6)
2 weeks	8.0±3.2	9.7±1.7	5.8±3.3	5.3±4.6	9.2±2.3	3.8±1.1
	(58.9±7.9)	(60.4±8.9)	(61.1±10.6)	(62.2±9.3)	(60.5±11.1)	(61.9±8.0)
1 month	8.9±7.1	4.2±5.9	8.4±8.9	9.1±7.3	7.2±6.6	10.0±11.2
	(58.2±3.2)	(55.3±6.1)	(59.8±4.7)	(58.5±9.2)	(59.9±11.9)	(59.9±12.4)
2 months	9.9±4.9	8.5±3.9	8.3±1.2	13.5±2.7	4.0±4.9	8.4±4.1
	(66.3±2.1)	(65.8±5.5)	(64.6±4.0)	(61.4±3.6)	(62.2±3.2)	(60.9±1.1)

[a]Micronuclei were counted in binucleated cells. Data are presented as the average number of micronuclei per 1000 binucleated cells, mean of 3 replicates ± SEM and, in brackets () as the % of binucleated cells, mean of 3 replicates ± SEM. The average value in the positive controls, i.e. cells exposed 24 h to 100 µM methane methylsulfonate (MMS), was 30.9±0.1. *: $p<0.05$ vs control (unexposed cells): differences were not statistically significant.

Table S6. mRNA expression of genes involved in DNA repair[a]

Time	NP (µg/mL)	TP53	ATM	ATR	APE1	PARP1	PCNA	XRCC1	POLB	LIG3
24 h	2.5	1.19±0.13	1.26±0.04	1.36±0.11	0.97±0.14	0.95±0.31	1.18±0.23	0.79±0.21	0.80±0.12	0.76±0.06
	10	1.32±0.25	1.34±0.18	1.48±0.22	1.12±0.14	0.77±0.56	1.36±0.17	1.61±0.59	1.31±0.25	1.29±0.40
	50	1.05±0.10	1.17±0.11	1.16±0.12	1.17±0.24	1.08±0.38	1.00±0.25	1.02±0.09	0.79±0.24	0.84±0.08
2 w.	2.5	1.07±0.23	1.14±0.18	1.24±0.48	0.74±0.07	0.87±0.06	0.94±0.38	0.67±0.10	1.12±0.52	1.07±0.13
	10	0.96±0.35	1.01±0.21	1.00±0.23	0.88±0.28	0.92±0.16	0.82±0.50	0.95±0.38	0.88±0.37	1.03±0.24
	50	0.93±0.36	0.92±0.22	0.89±0.16	0.79±0.12	0.83±0.08	0.73±0.37	0.92±0.39	0.87±0.43	1.14±0.43
1 m.	2.5	1.19±0.11	1.04±0.20	1.14±0.24	0.85±0.24	0.93±0.24	0.98±0.09	1.66±0.67	1.09±0.15	1.28±0.09
	10	1.03±0.25	0.85±0.18	0.91±0.14	0.80±0.13	0.79±0.12	0.67±0.14	1.18±0.37	1.02±0.45	1.01±0.23
	50	1.06±0.09	0.85±0.14	0.86±0.13	0.76±0.13	0.78±0.07	0.64±0.10	1.10±0.05	1.09±0.17	1.01±0.20
2 m.	2.5	1.03±0.50	1.32±0.66	1.17±0.11	0.84±0.14	0.82±0.15	0.90±0.37	0.70±0.16	0.99±0.51	0.76±0.22
	10	0.95±0.23	0.93±0.17	1.08±0.42	0.88±0.17	0.78±0.16	0.70±0.14	0.87±0.15	0.86±0.32	0.96±0.19
	50	0.79±0.23	0.78±0.22	0.80±0.14	0.78±0.17	0.82±0.10	0.60±0.21	0.55±0.26	0.68±0.29	0.65±0.24

[a] Gene expression was measured by RT-qPCR on A549 cells exposed for 24 h. 2 weeks (2 w.). 1 month (1 m.) or 2 months (2 m.) to 0. 2.5. 10 or 50 µg/mL TiO_2-NP. Results are expressed as $2^{-\Delta\Delta Cq}$ calculated with the reference gene GAPDH. Mean of four replicates ± standard error. *: $p<0.05$ vs control (unexposed cells): differences were not statistically significant.

References

Beers RF, Jr., Sizer IW. 1952. A spectrophotometric method for measuring the breakdown of hydrogen peroxide by catalase. J Biol Chem 195(1): 133-40.

Carlberg I, Mannervik B. 1985. Glutathione reductase. Methods Enzymol 113: 484-90.

Dorier M, Brun E, Veronesi G, Barreau F, Pernet-Gallay K, Desvergne C, Rabilloud T, Carapito C, Herlin-Boime N, Carriere M. 2015. Impact of anatase and rutile titanium dioxide nanoparticles on uptake carriers and efflux pumps in Caco-2 gut epithelial cells. Nanoscale 7(16): 7352-60.

Paglia DE, Valentine WN. 1967. Studies on the quantitative and qualitative characterization of erythrocyte glutathione peroxidase. J Lab Clin Med 70(1): 158-69.

Paoletti F, Aldinucci D, Mocali A, Caparrini A. 1986. A sensitive spectrophotometric method for the determination of superoxide dismutase activity in tissue extracts. Anal Biochem 154(2): 536-41.

Pfaffl MW, Tichopad A, Prgomet C, Neuvians TP. 2004. Determination of stable housekeeping genes, differentially regulated target genes and sample integrity: BestKeeper--Excel-based tool using pair-wise correlations. Biotechnol Lett 26(6): 509-15.